Supporting Information

Tuning Structure and Photoinduced Linkage Isomerism of Tetrapyridine Nitrosyl Ruthenium(II) Complexes by Changing of the *trans*-to-NO Coordinated Ligand

Vasily Vorobyev[a,b,c,*], Artem A. Mikhailov[a,b], Vladislav Yu. Komarov[a,b], Alexander N. Makhinya[a,b], Gennadiy A. Kostin[a,b]

[a]Nikolaev Institute of Inorganic Chemistry, Siberian Branch of the Russian Academy of Science, Novosibirsk, 630090, Russia

[b]Novosibirsk State University, Novosibirsk, 630090, Russia

[c]Department of Chemistry and the Center for Photochemical Sciences, Bowling Green State University, Bowling Green, OH 43402, USA

[*]Corresponding author: vasily.vorob@gmail.com

Figure S1

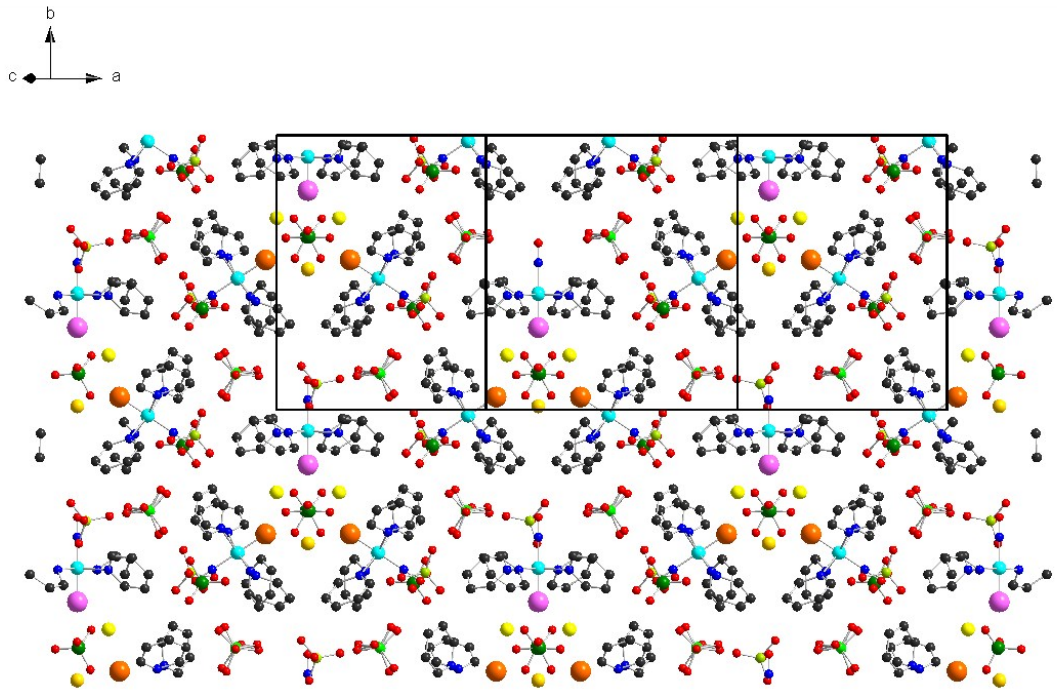

. Pseudo-hexagonal package of hydrogen-bonded ruthenium cations in the structure of $[RuNOPy_4OH](ClO_4)_2 \cdot H_2O$.

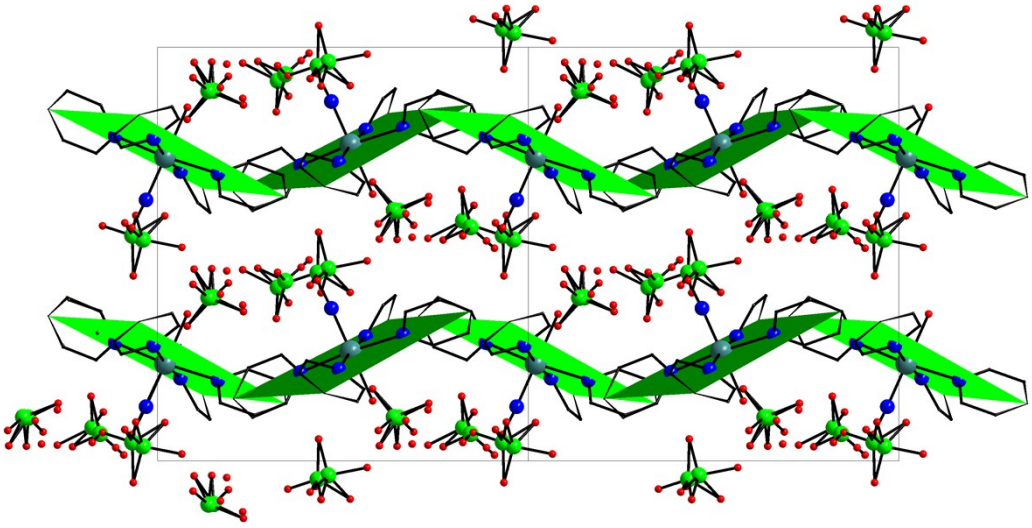

The package of layers in the structure of $[RuNOPy_4H_2O](ClO_4)_3 \cdot 2H_2O$.

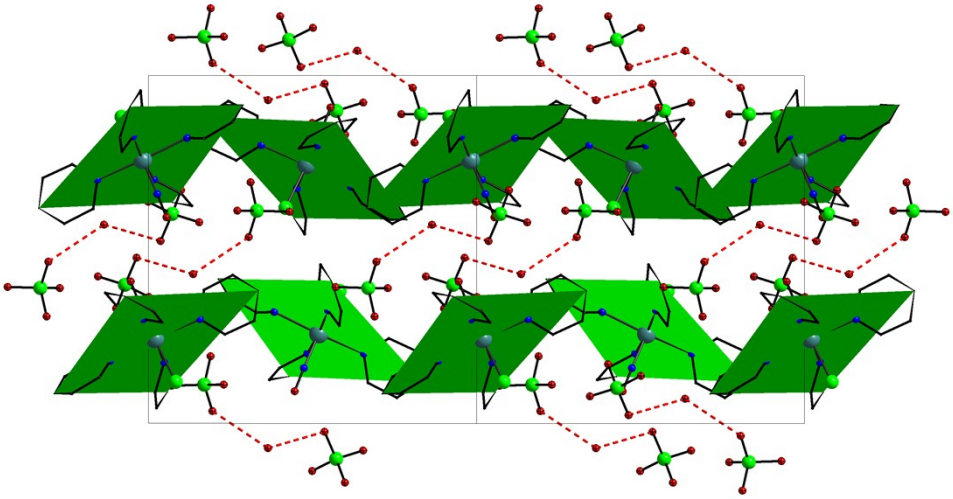

The package of layers in the structure of $[RuNOPy_4Cl](ClO_4)_2 \cdot H_2O$. Hydrogen bonds between perchlorate anions and water molecules are shown in dash.

Table S1. Selected geometrical parameters and vibrational frequencies (cm^{-1}) of $[RuNOPy_4X]^{n+}$ complexes for X = OH^-, Cl^-, and H_2O calculated in the gas phase.

	GS, Ru-NO			MS1, Ru-ON		
	1, G	**2**, W	**3**, Cl	**1**, G	**2**, W	**3**, Cl
Ru-NO	1.783	1.752	1.778	1.868	1.843	1.869
N-O	1.153	1.138	1.149	1.153	1.139	1.149
Ru-Py	2.098	2.103	2.104	2.088	2.094	2.094
Ru-X	1.931	2.099	2.278	1.910	2.058	2.245
mean Py tilt	54.1	43.8	46.4			
Ru shift	0.130	0.142	0.095			
$\nu(NO)_{DFT}$	1916	1999	1931	1837	1902	1846
$\nu(NO)_{exp}$	1873	1933	1906	1728	1780	1766

Table S2. Molecular orbitals in the ground and metastable states of complex **3** $[RuNOPy_4Cl]^{2+}$.

GS			MS1		
Energy, eV	Occ.	Scheme	Energy, eV	Occ.	Scheme
-14.059	2	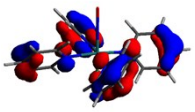	-14.071	2	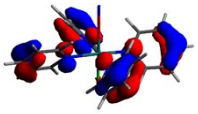
-13.961	2	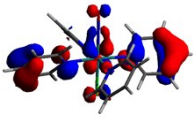	-13.908	2	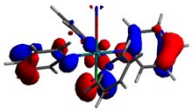
-13.953	2	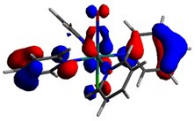	-13.899	2	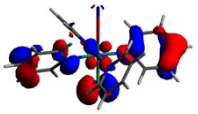
-13.708	2	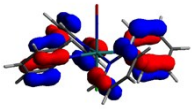	-13.693	2	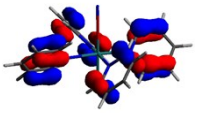
-13.653	2	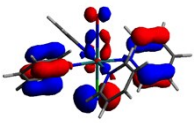	-13.491	2	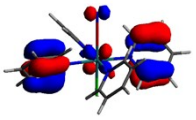
-13.650	2	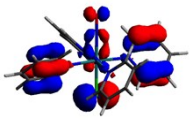	-13.486	2	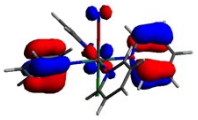
-13.342	2	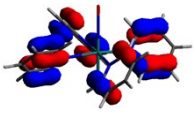	-13.330	2	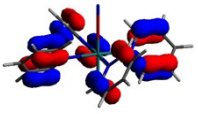
-13.130	2	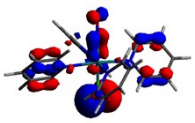	-12.980	2	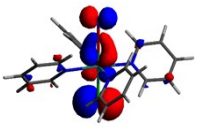
-13.129	2	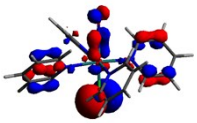	-12.979	2	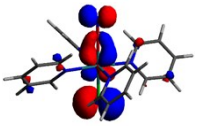
-12.972	2	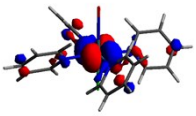	-12.762	2	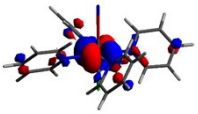
-10.573	0	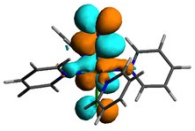	-11.128	0	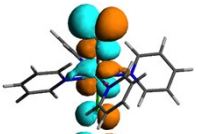
-10.572	0	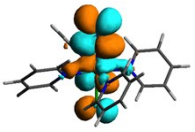	-11.127	0	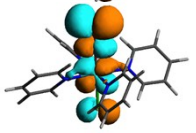
-9.231	0	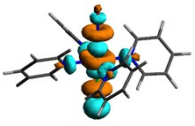	-9.307	0	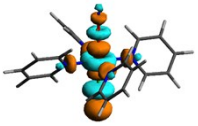
-9.013	0	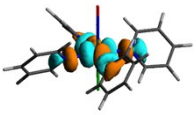	-8.804	0	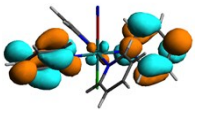

-8.817	0	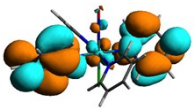	-8.799	0	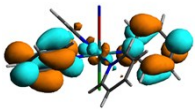
-8.812	0	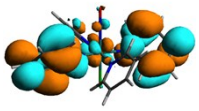	-8.790	0	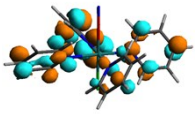
-8.800	0	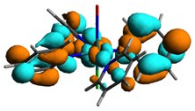	-8.782	0	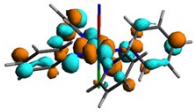
-8.796	0	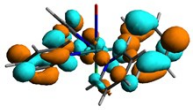	-8.689	0	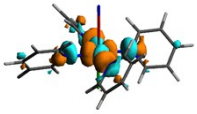
-8.404	0	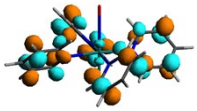	-8.428	0	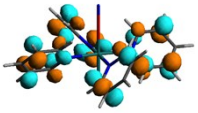
-8.106	0	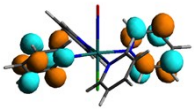	-8.106	0	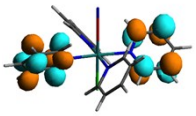

Table S3. The excitation energy (eV), oscillator strength (times 10^3), and transition of the electron density between molecular orbitals of the computed TD-DFT transitions in complexes **1**-**3** and their metastable states.

1, $[RuNOPy_4OH]^{2+}$

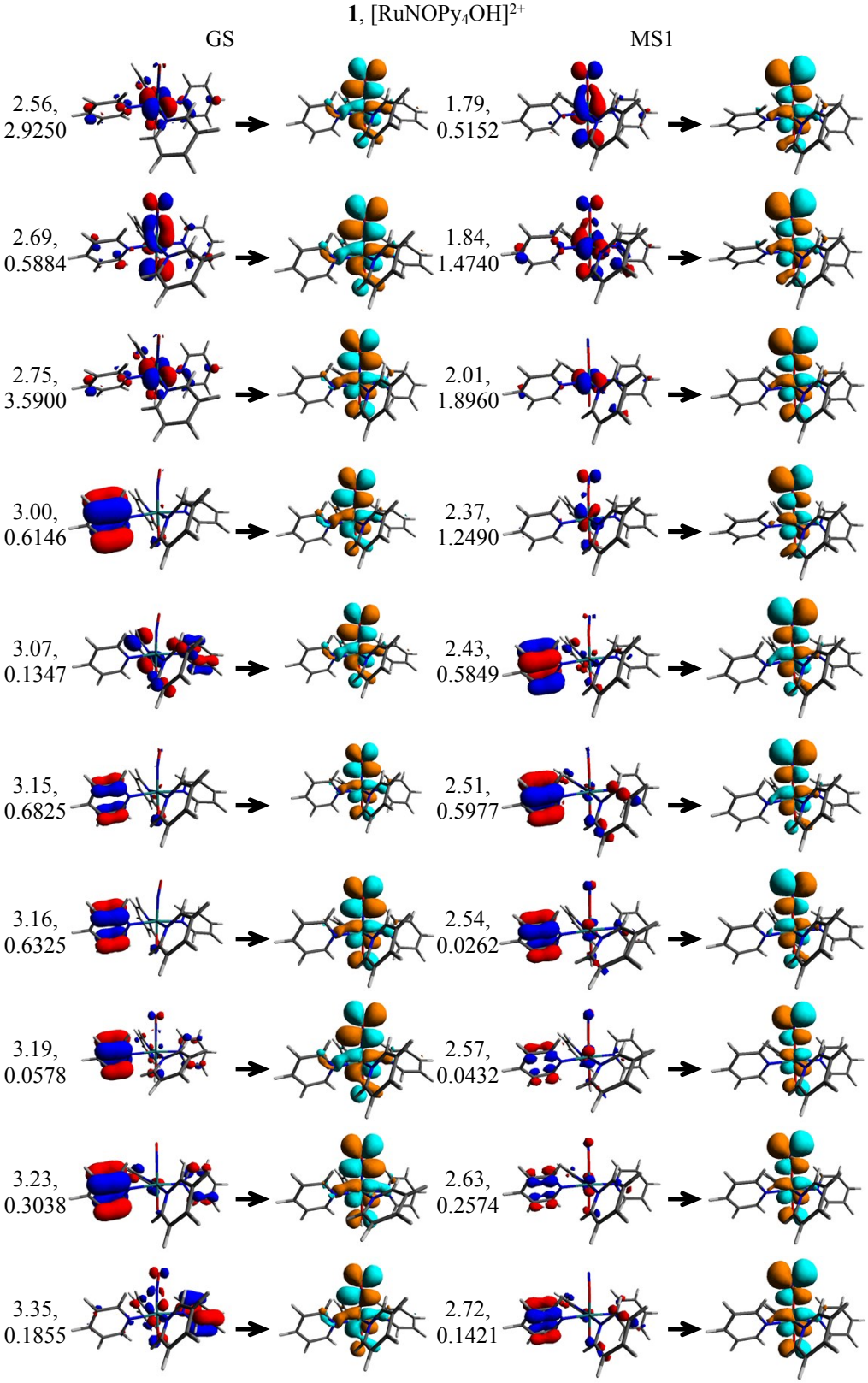

2, $[RuNOPy_4H_2O]^{3+}$

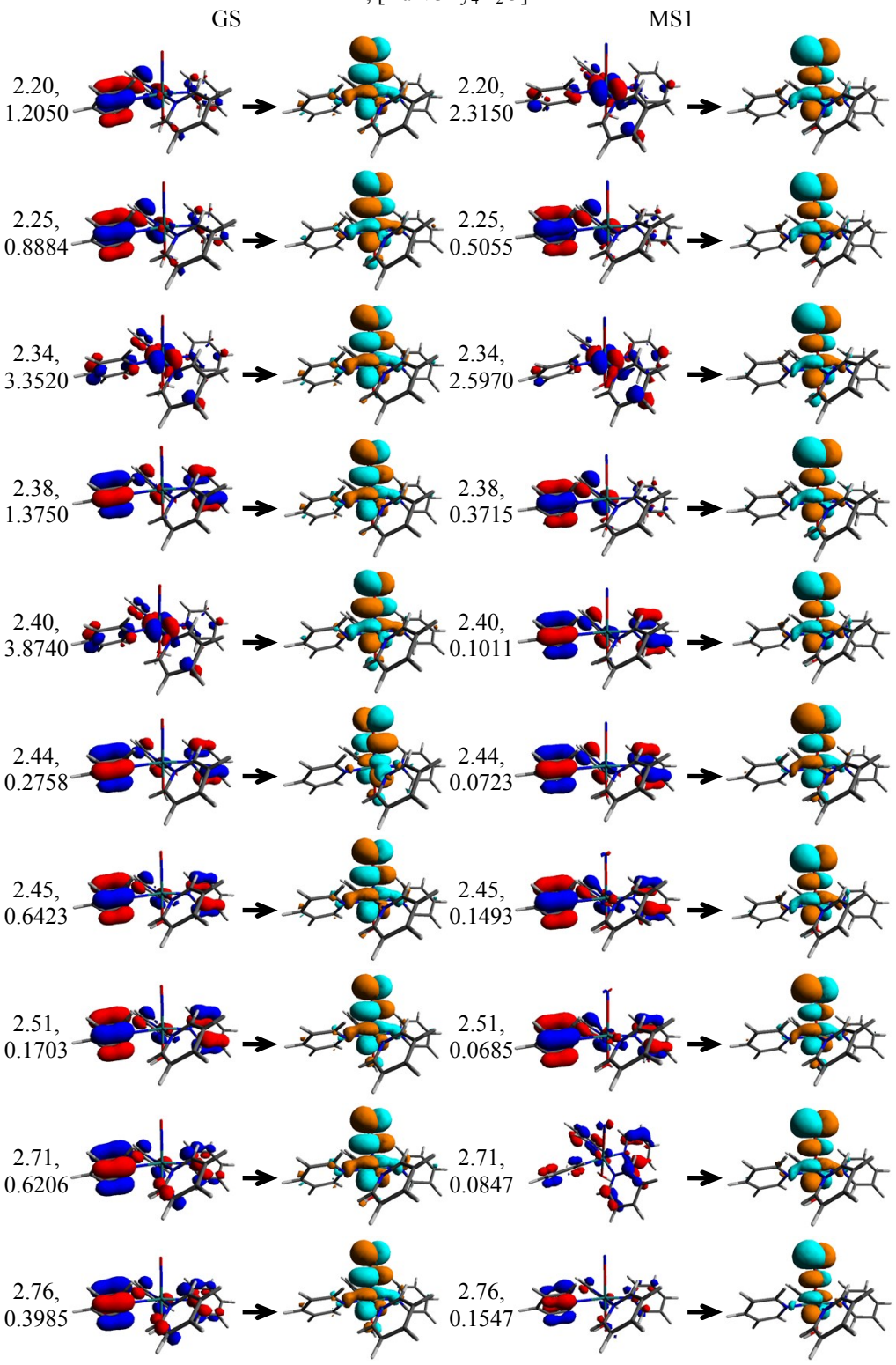

3, $[RuNOPy_4Cl]^{2+}$

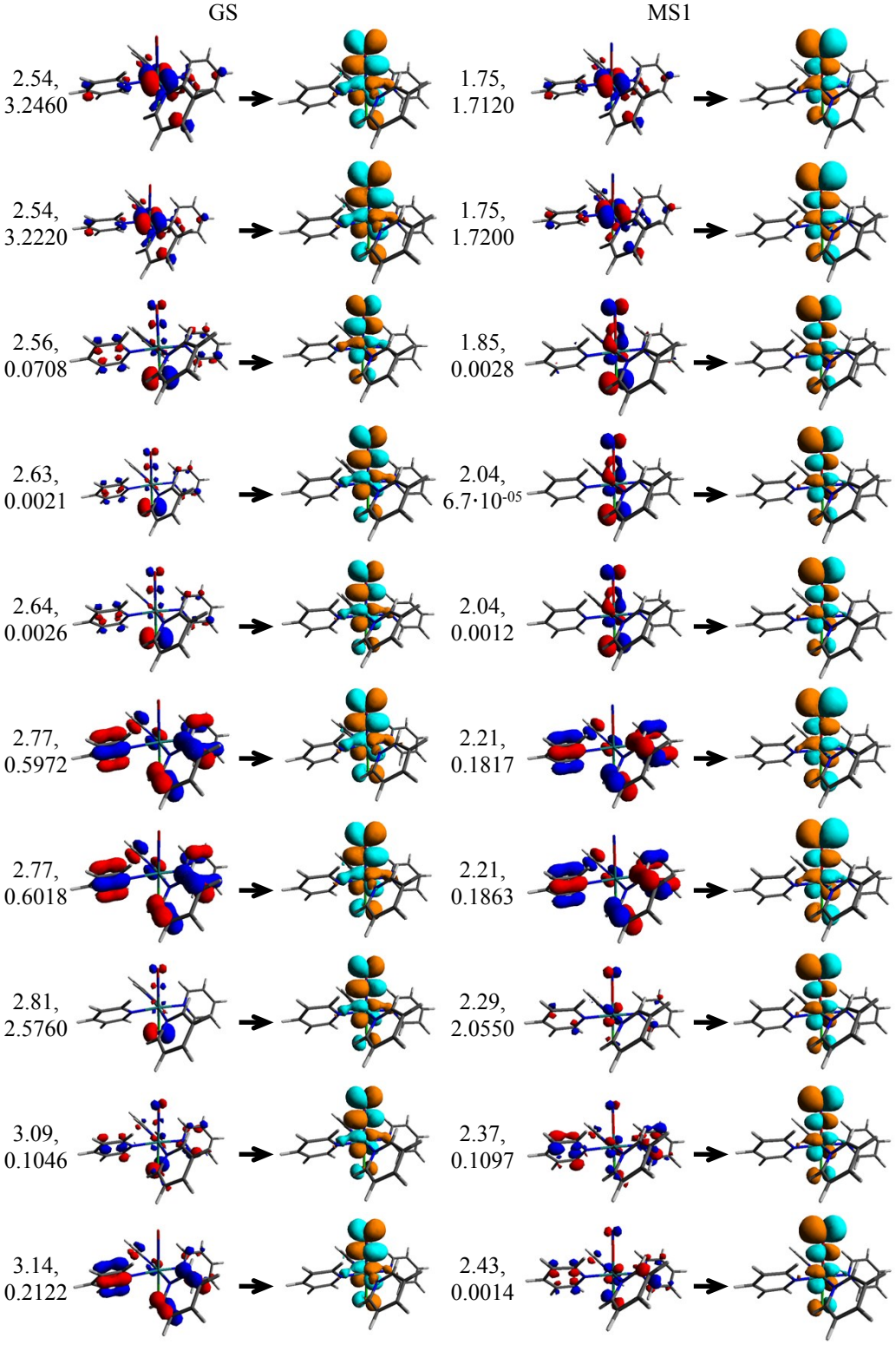

Fig. S2. The normalized ν(NO) absorption of the studied Ru-ON mixture in blue, red, and green data points from left to right, respectively. For the compound **1**, the complexes are *fac*-$K_2[RuNO(NO_2)_2Cl_3]$, *trans*-$[RuNOPy_4OH](ClO_4)_2 \cdot H_2O$ (**1**), and $[RuNO(NH_3)_5]Cl_3$. For the compound **2**, the complexes are *trans*-$[RuNO(NH_3)_4OH]Cl_2$, $[RuNO(NH_3)_5]Cl_3$, and *trans*-$[RuNOPy_4H_2O](ClO_4)_3 \cdot H_2O$ (**2**). Note that blue data points from *trans*-$[RuNO(NH_3)_4OH]Cl_2$ are contaminated by the *trans*-$[RuNOPy_4OH](ClO_4)_2 \cdot H_2O$ (**1**). For the compound **3**, the complexes are *cis*-$Cs[RuNO(NH_3)Cl_4] \cdot H_2O$, *trans*-$[RuNOPy_4Cl](ClO_4)_2 \cdot H_2O$ (**3**), and $[RuNO(NH_3)_5]Cl_3$.

Complex **1**, first sample

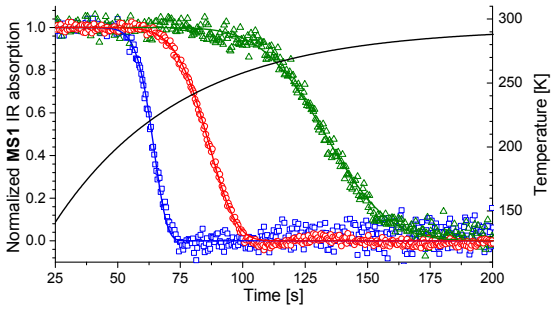

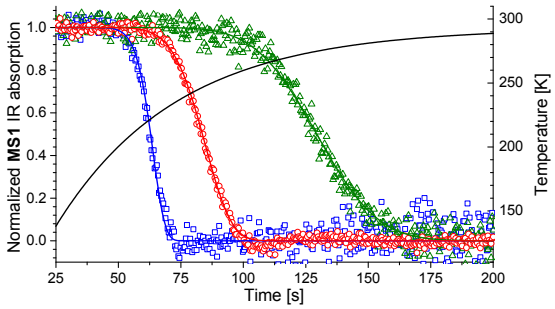

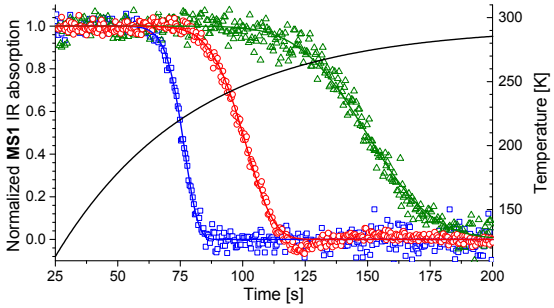

Complex **1**, second sample

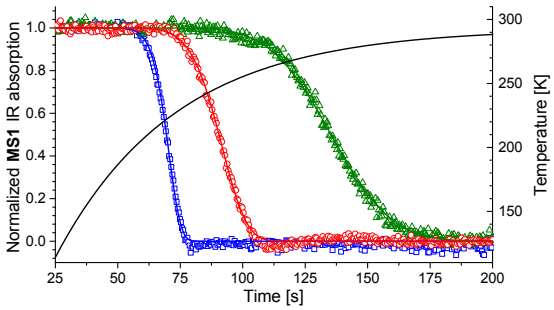

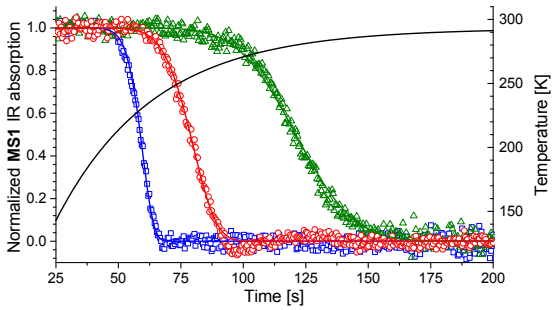

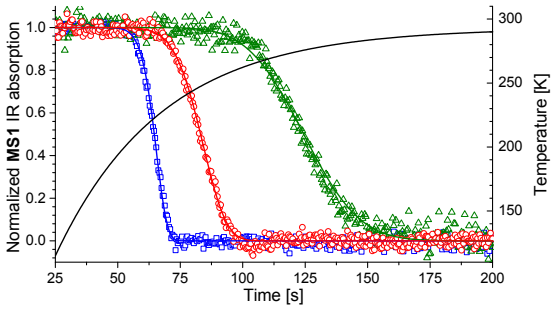

Complex **2**, first sample

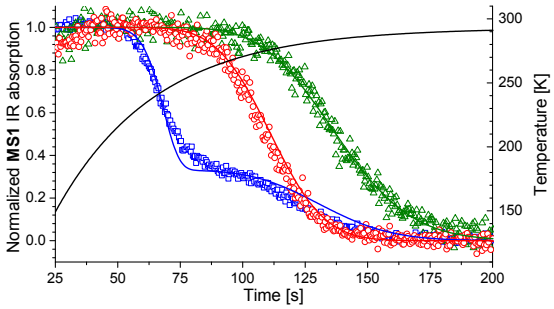

Complex **2**, second sample

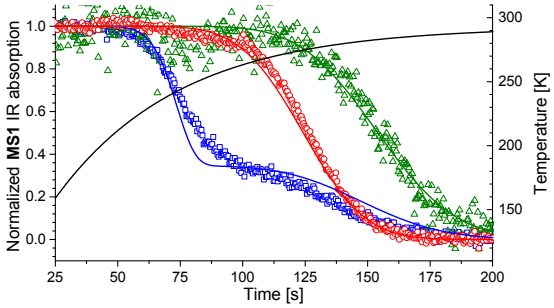

Complex **3**, first sample

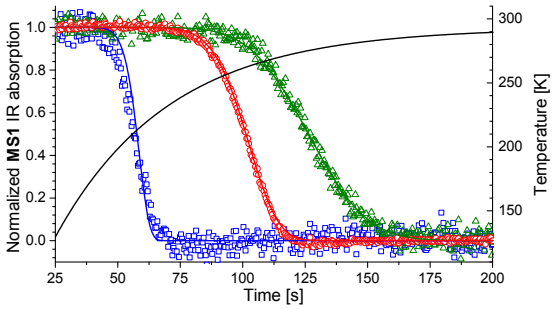

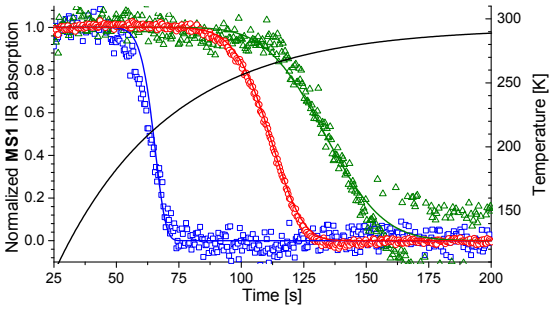

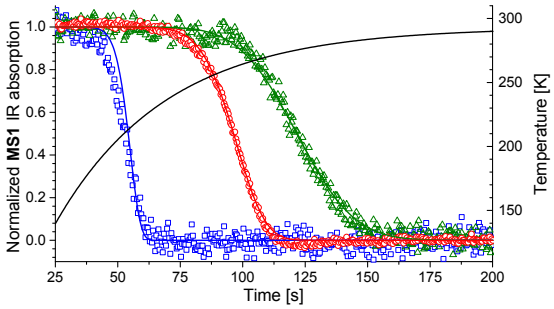

Complex **3**, second sample

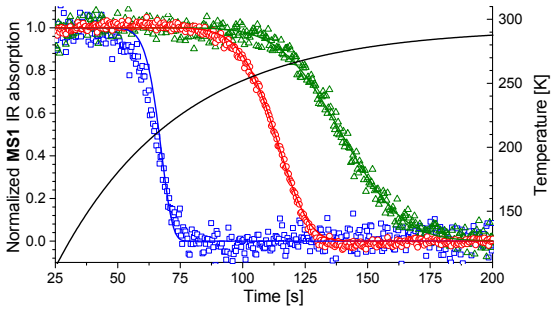

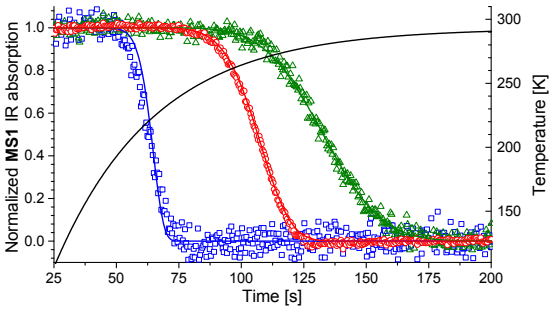

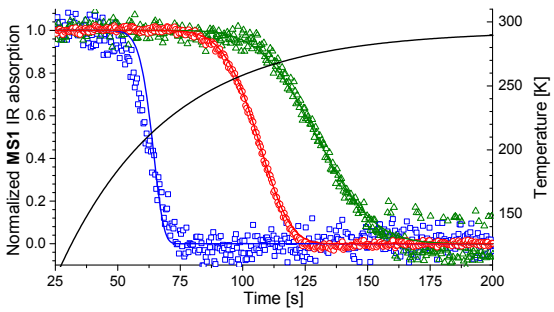

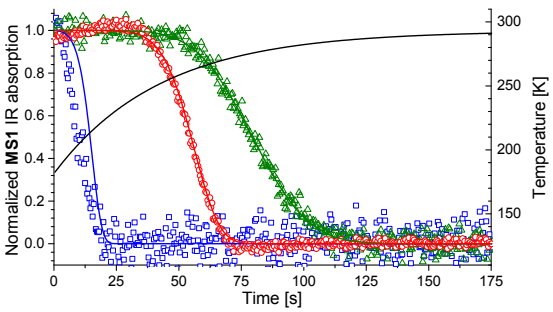

Fig. S3. Isothermal kinetic of MS1 – GS transformation for $[RuNO(Py)_4OH](ClO_4)_2 \cdot H_2O$. The sample pellet was cooled in a cryostat to 80 K, irradiated by 445 nm 100 mW LED. Next, the sample was heated to a specific temperature and the MS1 absorption band was monitored over time. The curves were treated as first-order kinetic. The activation parameters were determined from the Arrhenius plot lnk – 1/(RT): E_a = 50.9 (7.5) kJ mol^{-1}, $lg(k_0)$ = 9.6(1.8). T_d = 212(3) K.

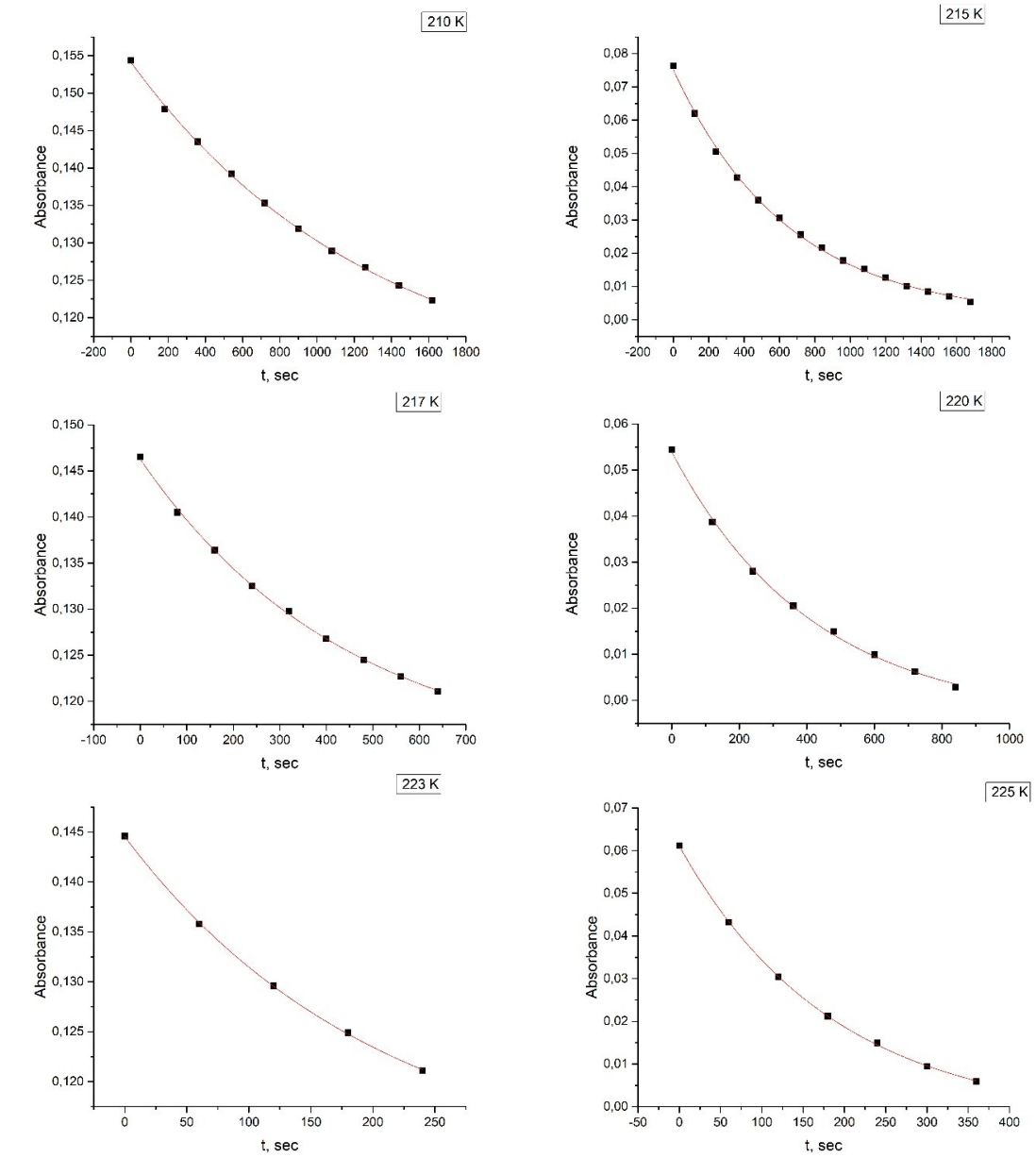

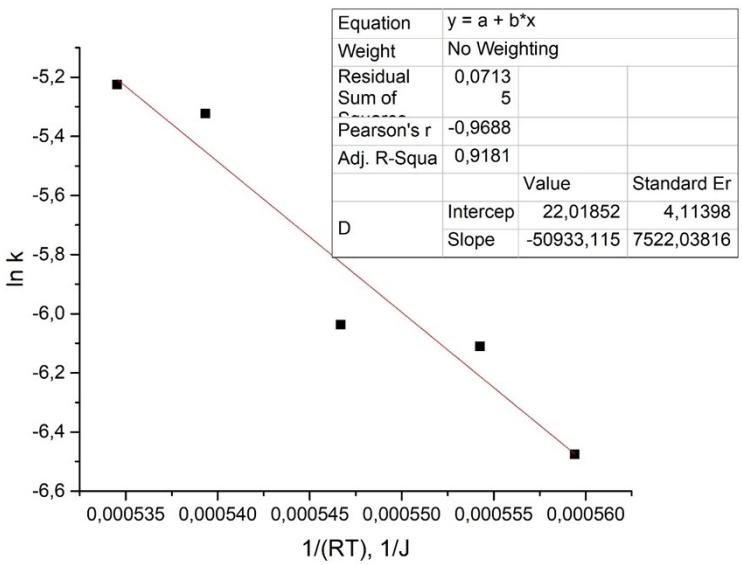

Fig. S4. The reaction cavities accessible for the atom nucleus of NO group in the complexes **1**-**3**. Z-axe is the direction of Ru-N-O.

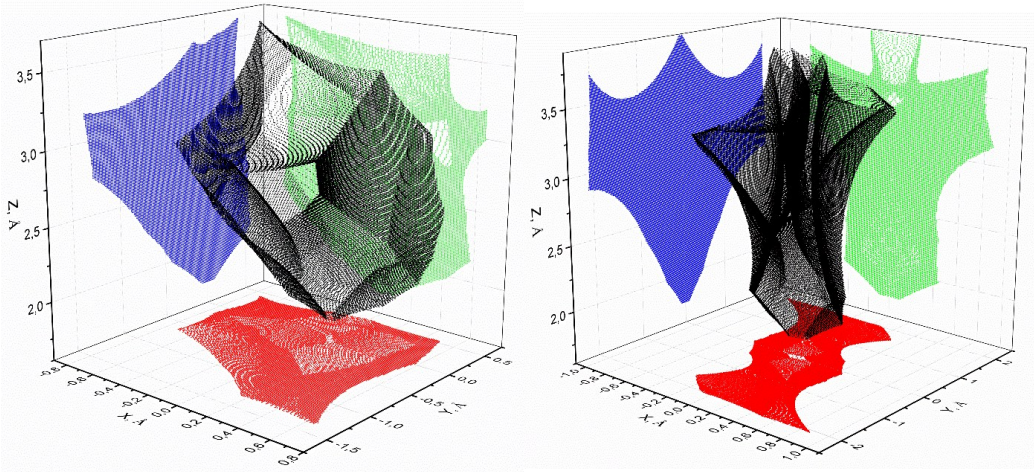

trans-[$RuNOPy_4OH$]$(ClO_4)_2 \cdot H_2O$ (**1**) – two symmetrically inequivalent fragments

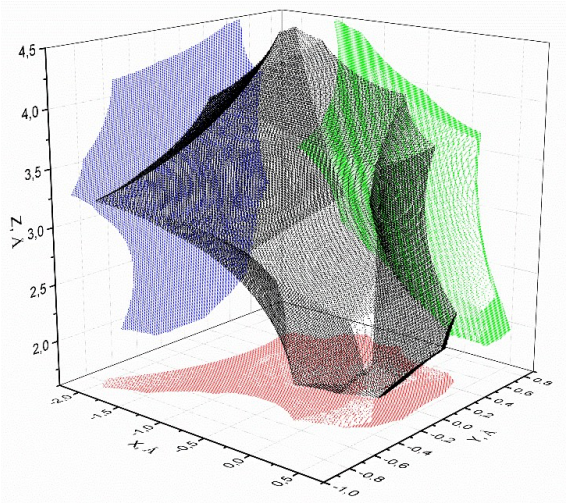

trans-[$RuNOPy_4H_2O$]$(ClO_4)_3 \cdot 2H_2O$ (**2**)

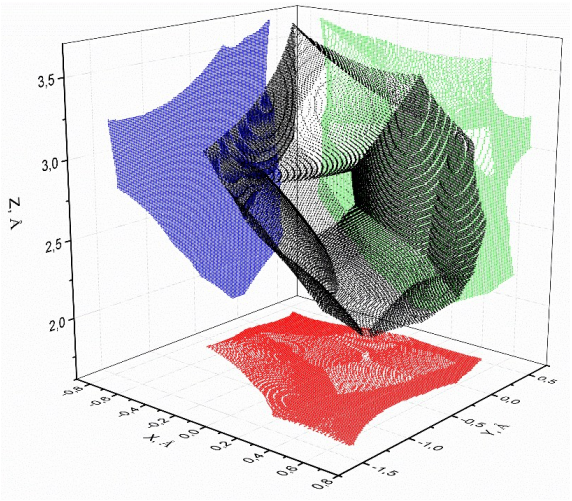

trans-[$RuNOPy_4Cl$]$(ClO_4)_2 \cdot H_2O$ (**3**)

Fig. S5. Voronoi-Dirichlet polyhedrons for the NO group in complexes **1-3**.

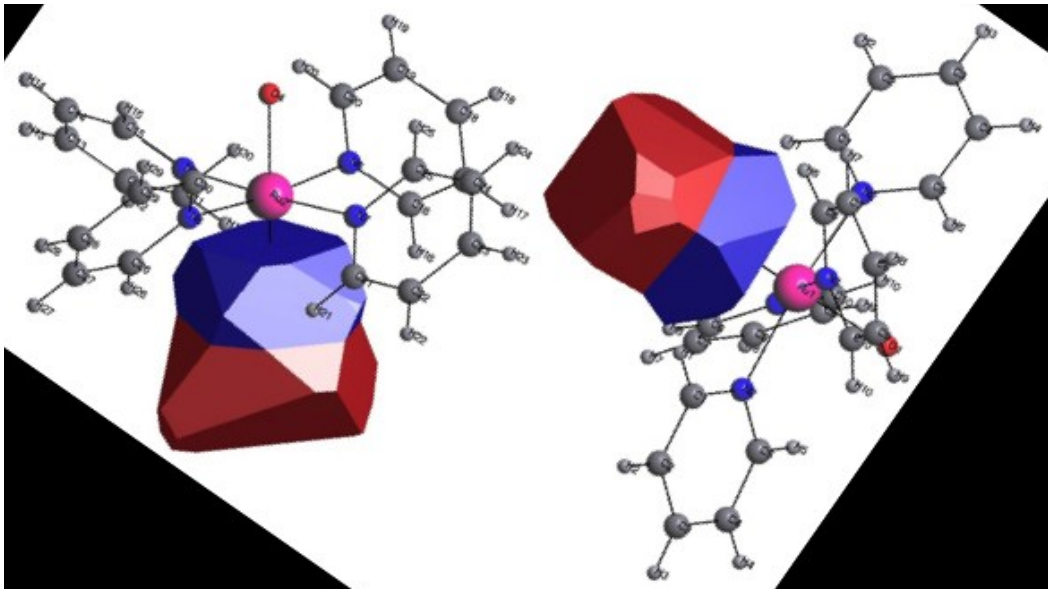

trans-[$RuNOPy_4OH$]$(ClO_4)_2 \cdot H_2O$ (**1**) – two symmetrically inequivalent fragments

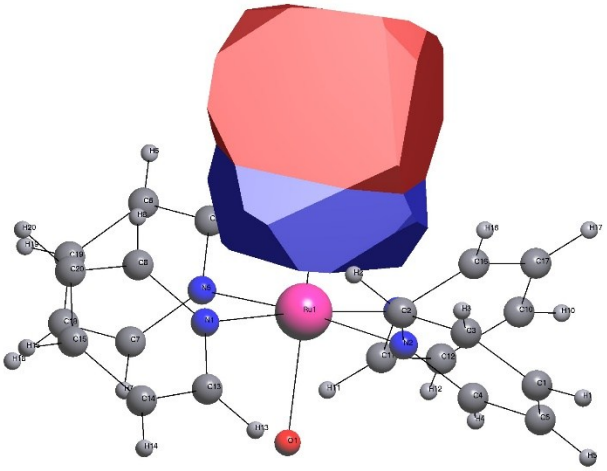

trans-[$RuNOPy_4H_2O$]$(ClO_4)_3 \cdot 2H_2O$ (**2**)

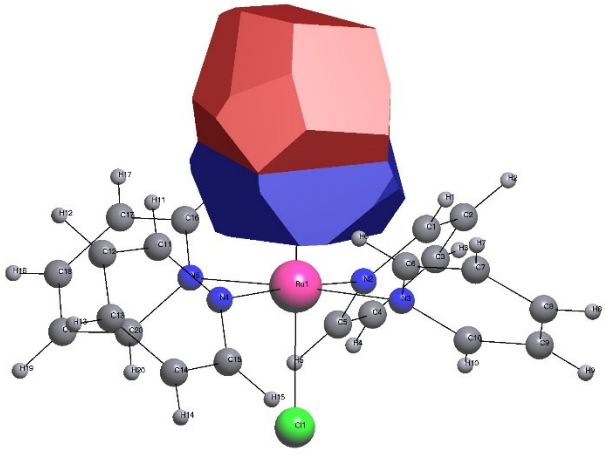

trans-[$RuNOPy_4Cl$]$(ClO_4)_2 \cdot H_2O$ (**3**)